Introduction to Aerospace Structures and Materials

Dr. ir. R.C. (René) Alderliesten

Introduction to Aerospace Structures and Materials

Introduction to Aerospace Structures and Materials

R.C. Alderliesten

7. Translating loads to stresses

7.1 Introduction

In the previous chapter, the loads acting on an aircraft or spacecraft structure have been discussed. These loads are generally considered to act at certain locations on the structure either by concentrated loads or by distributed loads. These loads induce deformations in the structure that correlate to stresses within the structure. To understand this, one should reconsider the example of the tensile test in chapter 1, where the load acting on the specimen induces an elongation (deformation) of the specimen, which corresponds to the stress in the specimen, calculated with the load divided by the cross section.

In this chapter, some cases are dealt with to explain how loads acting on an aircraft or spacecraft structure will induce deformation, but also lead to stresses within the structure. These stresses must be known, to be able to assess whether the materials used in the structure are capable to sustain the loads. Here, the stresses calculated from the loads acting on the structure should be compared with the stress-strain response of the materials to identify whether sufficient strain is present, and whether the material's stiffness will be sufficient to limit deformations to acceptable levels.

7.2 Pressurization of a fuselage structure

As commercial aircraft commonly operate at altitudes of 10000 meters, aircraft fuselages are pressurised to ensure that crew and passengers can breath normally. In this section the stresses induced into the structure as a result are explained.

7.2.1 Stresses in cylindrical pressure vessel

The circumferential and longitudinal stresses in a pressure vessel can be derived from equilibrium within the vessel. To calculate the circumferential stress, one first considers the upper half of a pressure vessel with unit length as illustrated in Figure 7.1.
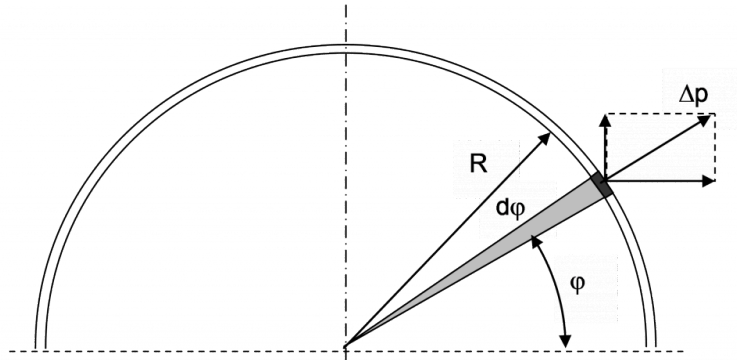

Figure 7.1
Equilibrium between radial pressure distribution and circumferential stress per unit vessel length. (TU Delft, n.d., 7-1.jpg. Own Work.)

There should be equilibrium in vertical direction between the circumferential stress σ_{circ} and the vertical component of the pressure p acting at the inner surface of the vessel. Per unit length[1] of the vessel, this equilibrium can be described with

$$2F_{circ} = 2\sigma_{circ}t = F_p \tag{7.1}$$

Goniometric analysis of the pressure difference (i.e. inside – outside) Δp acting on an element $d\phi$ implies that the vertical components of the radial pressure per unit length is given by

$$(7.2)$$

$$F_p = \int_0^\pi \Delta p \sin \phi R d\phi = \Delta p R \int_0^\pi \sin \phi d\phi = \Delta p R[- \cos \phi]_0^\pi = \Delta p R$$

---

1. Per unit length means that the parameter L describing the length of the pressure vessel is set equal to 1. It therefore can be neglected in equations (7.1) and (7.2). One should be aware however, that the correct relation between load and stress is given by a cross sectional area (length x thickness) rather than just thickness.

Combining equation (7.1) and equation (7.2) then implies that:

$$2\sigma_{circ}t = \Delta pR \tag{7.3}$$

To calculate the stress in longitudinal direction, the pressure vessel should be considered as illustrated in Figure 7.2. The pressure $d\phi$ acting on the circular surface should be in equilibrium with the longitudinal stress acting at the circumference of the vessel.
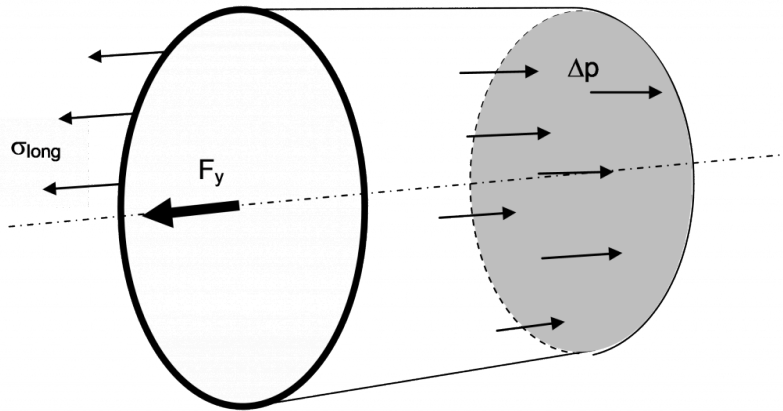
Figure 7.2
Illustration of equilibrium of the internal pressure and the longitudinal stress. (Alderliesten, 2011, 7-2.jpg. Own Work.)

The equilibrium is given by:

$$F_{long} = 2\pi R\sigma_{long}t = \Delta p\pi R^2 = F_p \tag{7.4}$$

Thus, the circumferential and longitudinal stresses in a pressure vessel can be described with:

$$\sigma_{circ} = \frac{\Delta pR}{t}$$
$$\sigma_{long} = \frac{\Delta pR}{2t} \tag{7.5}$$

Following from chapter 1 and equation (1.11), the Hooke's law for the bi-axial stress condition (plane stress) in a pressure vessel is then described by:

$$\varepsilon_{circ} = \frac{\sigma_{circ}}{E} - \nu\frac{\sigma_{long}}{E}$$
$$\varepsilon_{long} = \frac{\sigma_{long}}{E} - \nu\frac{\sigma_{circ}}{E} \tag{7.6}$$

Equation (7.5) implies that the circumferential stress is twice the longitudinal stress. Combining equation (7.5) and equation (7.6) this results in:

$$\varepsilon_{circ} = \frac{\sigma_{circ}}{E}\left(1 - \frac{\nu}{2}\right)$$
$$\varepsilon_{long} = \frac{\sigma_{long}}{E}(1 - 2\nu) \tag{7.7}$$

For a metallic pressure vessel the Poisson's ratio is about 0.3, which means that with equation (7.7) the circumferential strain is about 4.25 times larger than the longitudinal strain.

7.2.2 Connection between cylinder and spherical end sections

Consider a metallic pressure vessel as indicated in Figure 7.3. In this figure several locations of interest can be identified: the weld lines between the individual metal plates and the transition from a tubular shape to the spherical end sections.
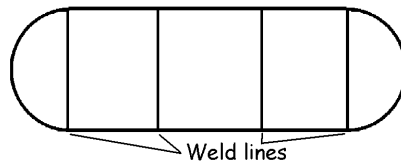
Figure 7.3
Illustration of a pressure vessel containing weld lines. (TU Delft, n.d., 7-3.jpg. Own Work.)

To address the strength of the weld lines in the tubular section, the longitudinal stress should be considered, because that is the stress perpendicular to the weld line pulling the welded components apart. Because the circumferential stress is twice the longitudinal stress, the weld lines should be oriented in circumferential direction, rather than longitudinal direction. Otherwise, the stress loading of the weld would be twice the stress loading of the weld in Figure 7.3 under the same pressurization.
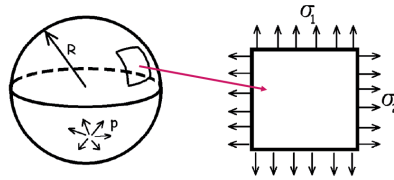
Figure 7.4
Illustration of a spherical pressure vessel. (TU Delft, n.d., 7-4.jpg. Own Work.)

To calculate the stress in the spherical end sections, first a pressurized sphere is considered, see Figure 7.4. In this vessel the stresses in both directions are equal to[2]:

$$\sigma_1 = \sigma_2 = \frac{\Delta pR}{2t} \tag{7.8}$$

With the Hooke's law for bi-axial loaded plates, see equation (1.11), this implies for the strains in both directions:

$$\varepsilon_{sphere} = \frac{\Delta pR}{2t}\frac{1}{E}(1-\nu) \tag{7.9}$$

To create the welded connection between the tubular section and the spherical sections in Figure 7.3, one should consider the question whether the thickness of both sections should be equal or not. In general, discontinuities in circumferential strain as illustrated in Figure 7.5 should be avoided, because they would lead to unwanted deformations, or even damage and/or failure. With the equations for strain given for both sections with respectively equation (7.7) and equation (7.9) , potential strain discontinuities can be assessed.
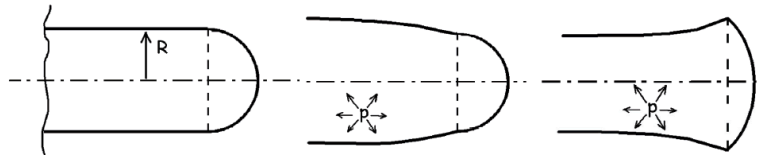

Figure 7.5
Illustration of the transition between tubular and spherical section without strain discontinuity (left) and with strain discontinuities (centre and right). (TU Delft, n.d., 7-5.jpg. Own Work.)

2. A similar derivation as presented in section 7.2.1 can be given for this case, except that it will be somewhat more complex. The analysis should be 3D instead of the 2D in Figure 7.1.

To derive the ratio between the thicknesses of both sections the circumferential strain should be equal to the strain in the spherical section, thus $\varepsilon_{circ} = \varepsilon_{sphere}$:

$$\varepsilon_{sphere} = \frac{\Delta pR}{2t}\frac{1}{E}(1 - \nu) = \frac{\Delta pR}{t}\frac{1}{E}(1 - \frac{\nu}{2}) = \varepsilon_{circ} \qquad (7.10)$$

This results in the following relation:

$$\frac{R_{sphere}}{R_{cylinder}} = \frac{2t_{sphere}(1 - \frac{\nu}{2})}{t_{cylinder}(1 - \nu)} = 1 \Rightarrow t_{sphere} = 0.41 t_{cylinder} \qquad (7.11)$$

In case the radii of both sections are identical this means that the thickness of the cylindrical section is 2.5 times the thickness of the spherical section.

7.2.3 Pressurization of an aircraft cabin structure

Of course, the example of a pressure vessel analyzed in the previous section is a simplified case compared to an aircraft fuselage structure under pressurization. Therefore, some remarks have to be made in addition to the previous analysis.

First of all, the thickness of the fuselage shells is not constant throughout the fuselage. Local reinforcement, especially near cut-outs such as doors and windows, will locally redistribute the stresses and change the deformation of the pressured shell structure.

In addition, it was already discussed in chapter 5 and 6 that the fuselage shell is reinforced by stringers and frames to maintain the aerodynamic shape under all operating conditions. Especially the frames have a significant impact on the deformation of the pressurized fuselage and as a consequence on the circumferential stresses. The contribution of the frames to the response of the fuselage to pressurization is illustrated in Figure 7.6.
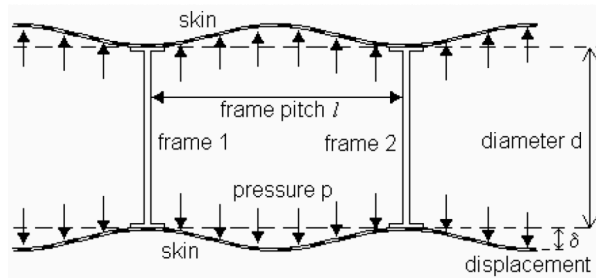
Figure 7.6
Illustration of frame contribution to the fuselage response to pressurization; a pillowing effect occurs due to limited deformation near the frames. (TU Delft, n.d., 7-6.jpg. Own Work.)

Because failure of the fuselage shell structure under pressurization may imply a disastrous occurrence similar to an exploding balloon, this type of fracture should be avoided at all times. First, the maximum pressurization load is defined to limit the static load that may occur, while secondly, damage retardant features are applied in the fuselage to stop cracks that may occur during over-pressurization.

Limit load cannot be defined for fuselage pressurization according to the formal definition, i.e. once in the lifetime of the aircraft, because the pressurization occurs every flight. For that reason, a larger safety factor is applied to the maximum pressurization load, often a factor 2 is applied.

In case of pressurization loads, the pressure differential is considered to induce the longitudinal and circumferential stress in the fuselage. This pressure differential is the difference between the inside pressure of the aircraft and the outside pressure. The design pressure differential is thus defined as:

$$\Delta p = p_d = p_{cabin} - p_h \qquad (7.12)$$

where p_{cabin} is the pressure inside the fuselage and p_h the pressure at an altitude h. For the cabin pressure often a pressure is taken at an altitude between 2400 and 3000 m, rather than the pressure at sea level. This pressure is considered to be still comfortable for the passengers, while it reduces the design pressure differential for a cruise altitude h.

This can be illustrated as follows. If a safety factor of 2 is applied, the maximum pressure differential is equal to 2 p_d. Assume that this maximum pressure differential is equal to 45 kPa. In case the maximum cruise altitude is set to be 9050 m, then a

cabin altitude of 2440 m could be used. However, if an aircraft altitude of 10350 m is required; this implies a cabin altitude of 3050 m, thus a lower cabin pressure.

7.3 Torsional loading of a fuselage structure

Another load case that may act on an aircraft fuselage is torsional loading. As explained in chapter 6, this may occur if the vertical tail of an aircraft is laterally loaded by gust wind, or by forces induced by the rudder. Aside from bending of the vertical tail, this load case will induce rotation of the rear fuselage section.

This section will discuss in more detail the torsional loading of a cylindrical fuselage section and the implications of such load case to the stresses within that structure.

If a torsional moment is applied to a cylindrical shell, stresses occur within that shell structure. To understand the nature of these stresses, one should first consider the shell to be non-continuous as illustrated in Figure 7.7. It is rather evident that the torsional moment will induce the deformation as shown at the left hand side of this figure. To prevent this deformation and to keep the longitudinal edges of the cylindrical shell positioned opposite to each other forces must be applied to these longitudinal edges in the opposite direction as the deformation.
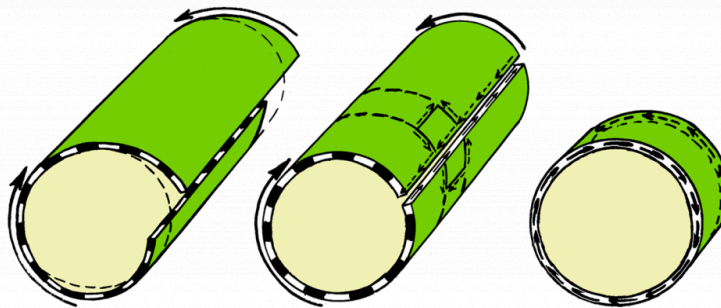

Figure 7.7
Illustration of a cylindrical shell loaded by torsion; in the case the shell is not continuous it deforms as shown left. To prevent that deformation shear stresses must occur. (TU Delft, n.d., 7-7.jpg. Own Work.)

These forces must be in equilibrium within the shell structures, which implies a shear stress acting in opposite direction as the applied moment, because these shear stresses should create equilibrium with the applied moment.
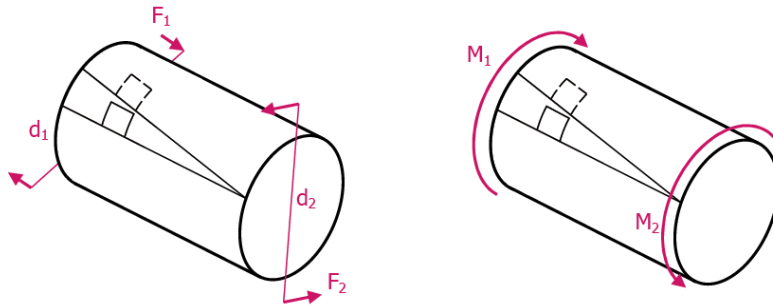

Figure 7.8
Illustration of the force-couple systems and torsional moments acting on a cylindrical shell. (Alderliesten, 2011, 7-8.jpg. Own Work.)

To identify these shear stresses and their direction, one may also look at the deformation of a cylinder deformed under a torsional moment. A rectangular section on such cylinder will deform into a parallelogram, as illustrated in Figure 7.8.

If equilibrium is satisfied in the example shown in Figure 7.8 this means that

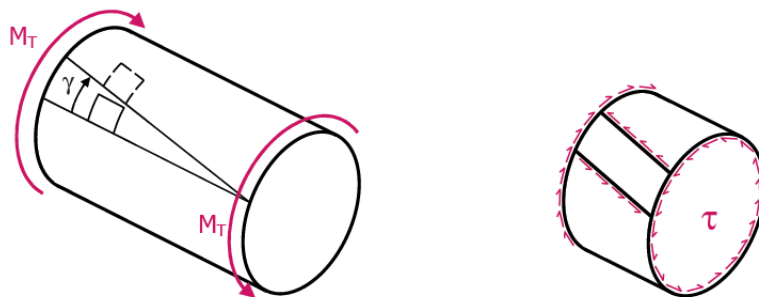$$F_1 d_1 = F_2 d_2 = F_n d_n \Rightarrow M_1 = M_2 = M_n \tag{7.13}$$

Figure 7.9
Illustration of the resulting shear stresses as a result of the torsional moments acting on a cylindrical shell. . (Alderliesten, 2011, 7-9.jpg. Own Work.)

Thus a torsional deformation induces shear stress according to equation (1.7), see Figure 7.9

$$\gamma = \frac{\tau}{G} \qquad (7.14)$$

If the shear stress acting in the shell with thickness t at a distance r from the centre of the cylinder over the complete circumference of the cylinder is in equilibrium with the torsional moment M_T (see right hand side of Figure 7.9), this means that

$$M_T = \tau 2\pi\, r\, tr = 2\tau\pi r^2 t \qquad (7.15)$$

Defining the shear flow q as $q = t\tau$, this equation can be written as

$$M_T = 2qA \qquad (7.16)$$

In other words, in case a thin walled structure like the fuselage shell structure is loaded by a torsional moment M_T then the shear flow in that shell is solely determined by the enclosed area A. This relationship appears to be independent of the shape of the enclosed area. Thus whether the area is a cylinder as in the example of a fuselage, or a wing box structure, as long as the area is equal, the shear flow q will be the same according to

$$q = \frac{M_T}{2A} \qquad (7.17)$$

This can be illustrated with a wing box as illustrated in Figure 7.10. Dividing the contour of the wing box structure in small elements, then for each element the fractional moment is given by

$$dM_T = q\, ds\, a = q2dA \qquad (7.18)$$

Superimposing all fractions together, one evidently gets equation (7.17).
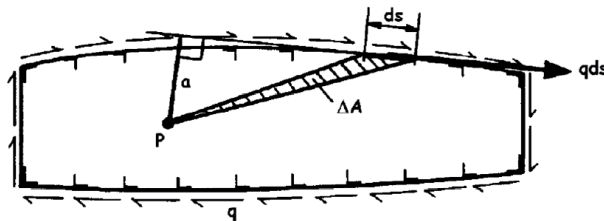

Figure 7.10
Illustration of a torsional moment M_T acting on a wing box structure causing shear flow q. (TU Delft, n.d., 7-10.jpg. Own Work.)
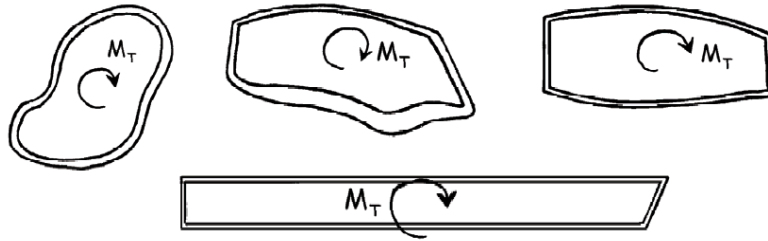
Figure 7.11
Arbitrary enclosed areas for thin walled structures under torsional moment M_T. (TU Delft, n.d., 7-11.jpg. Own Work.)

Thus all structures illustrated in Figure 7.11 have the same shear flow under torsional moment M_T independent of the cross sectional shape. This closed section is therefore often called a torsion box, because it resists torsional deformation efficiently.With the above discussion, it can be concluded that a torsional moment is resisted by shear stresses within the thin walled shell structure. However, in case a cut-out is created within such structure, for example a door or window in an aircraft fuselage, the torsional box will not function well at the location of the cut-out. This is illustrated in Figure 7.12. For this reason cut-outs must be reinforced locally around the cut-out to provide the resistance against shear deformation that was provided by the removed shell structure. This is often created by locally increasing the thickness with doublers and stiff frames and stringers providing rigid corners.
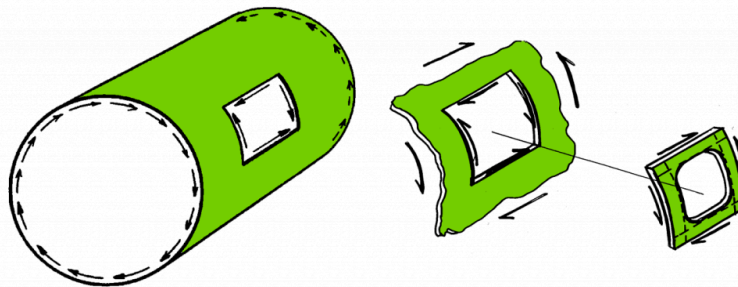

Figure 7.12
Cut-out in cylindrical shell under torsion must be reinforced to provide resistance against shear deformation. (TU Delft, n.d., 7-12.jpg. Own Work.)

7.4 Bending of a wing structure

It was explained in chapter 5 that wing bending is taken up primarily by the spars in that wing structure. In this section the function of the spar and its structural elements is explained in more detail and a structural analysis is performed

7.4.1 Shear deformation

First an elementary spar is considered as illustrated in the left hand side of Figure 7.13. The loads acting on that spar structure impose a diamond shaped deformation that is resisted by the sheets, see section 5.5.2. Assuming that the bars or the girders are stiff and rigid prohibiting any (bending) deformation, then the girders exercise shear stresses on the sheets and in return (for equilibrium) the sheets induce shear stresses on the girders, see Figure 7.14

The consequence is that if the sheets are being removed, the frames will not be capably of resisting the deformation, which corresponds to the explanation in section 5.3.2.
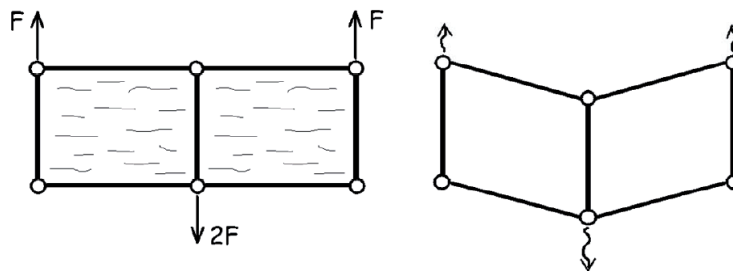

Figure 7.13
Elementary spar constructed from rigid girders and sheets (left) will deform if sheets are removed (right). . (TU Delft, n.d., 7-13.jpg. Own Work.)
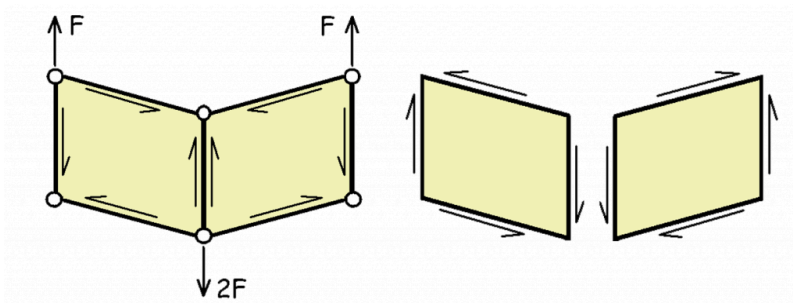
Figure 7.14
Illustration of shear stresses in the girders induced by the sheets (left) and the equilibrium shear stresses in the sheets (right). (TU Delft, n.d., 7-14.jpg. Own Work.)

The resistance to shear deformation is in fact the resistance to tension and compression under 45 degrees. To relate the shear deformation to the tensional and compressive deformation, the relationship between E, ν, G should be used, see section 1.6.

At certain levels of the applied forces F, the shear stress in the sheets will reach a critical level resulting in pleat or wrinkle formation within the sheets. These pleats are often referred to as shear buckling of the sheets. However, one should not consider this as failure, because the diagonal function is still maintained by the sheets. In other words, the structure still functions well, and if the loads are removed the pleats will usually disappear (i.e. when the buckling is elastic).

7.4.2 Stress analysis: breaking-up structural elements

To analyse a spar structure and to calculate the stresses induced by the applied load, the spar must be broken-up into individual elements. An example for a single spar element structure loaded by force F is given in Figure 7.15. For this example, equilibrium must be satisfied, which is used to calculate the reaction forces in the structural elements.
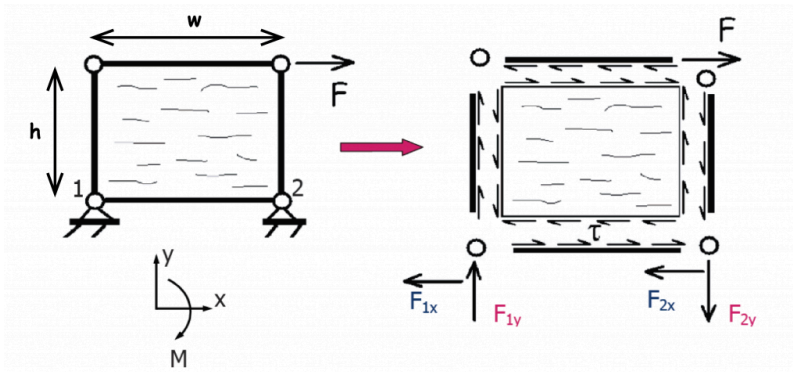
Figure 7.15
Single spar element loaded by force F (left) broken up into individual spars and sheet with reaction forces (right).
(TU Delft, n.d., 7-15.jpg. Own Work.)

For example, equilibrium in horizontal direction yields when:

$$F - F_{1x} - F_{2x} = 0 \tag{7.19}$$

while equilibrium in vertical direction is satisfied when:

$$F_{1y} - F_{2y} = 0 \tag{7.20}$$

The relation between the horizontal and vertical forces is given by the moment equilibrium.

Assume that the spar element in Figure 7.15 has a height h and a width w, then equilibrium of moments about location 2 implies that:

$$Fh + F_{1y}w = 0 \tag{7.21}$$

Subsequently, the equilibrium in each element can be evaluated. For example, the upper horizontal spar element is loaded at the right hand side by a force F, which can only be kept in equilibrium by the shear forces induced by the sheet over the length w of the spar element. This means that the normal stress at the right hand side of the element is equal to the applied force F and gradually decreases to zero to the left side of the element. Thus the shear stress τ in the sheet is in equilibrium with the normal forces in the frames.

An important remark must be made. Considering loading of elements, then tension and compression imply a physical difference, which easily can be related to a sign convention; tension is positive and compression negative. However, for shear deformation there is physically no difference between both deformations, see Figure

7.16. This means that for the analysis of spar bending a sign convention must be agreed upon like for instance illustrated in Figure 7.16.

Be aware however, that despite tension and compression are easily captured by respectively a positive and a negative sign, this assumes that both cases are identical but opposite of sign. However, physically tension may be considered being different from compression. Consider for example the presence of a crack. Under tension the crack would open and all load has to bypass the crack, while in compression the crack closes, enabling the load to be transferred through the crack.
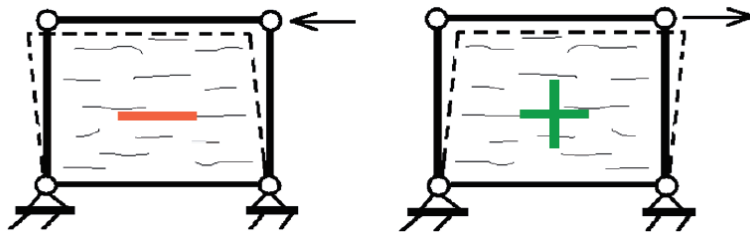

Figure 7.16
A sign convention for shear is needed to analyse the spar deformation. (TU Delft, n.d., 7-16.jpg. Own Work.)

From the above explanation it is evident that the in case of bending, the shear function of spar webs is essential. However, the webs have to be supported on the upper and lower side by caps or girders in order to realize equilibrium. In this configuration, the webs transfer (external) transverse forces into shear-flows, while the caps transfer shear-flows in normal forces.

7.5 Case study: bending of wing spar

To illustrate the previous explanation, this section discusses the approach for a simplified wing spar loaded in bending, illustrated in Figure 7.17.

7.5.1 Normal and shear forces

The general approach to this problem is to first check the global equilibrium of the problem. This means that the reaction forces at the spar root, i.e. at the clamping area (see Figure 7.18), should provide equilibrium with the external forces F_i.
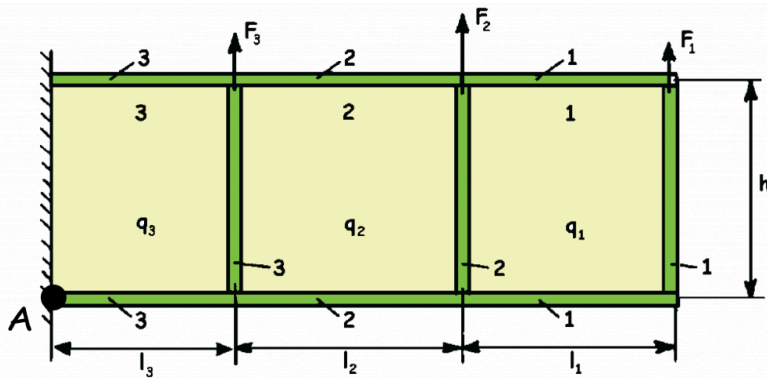

Figure 7.17
Simplified wing spar loaded by forces F_1 to F_3. (TU Delft, n.d., 7-17.jpg. Own Work.)

Global equilibrium implies in (horizontal) x-direction that

$$N_{U_4} - N_{L_4} = 0 \tag{7.22}$$

And in y-direction

$$F_1 + F_2 + F_3 + q_3 h = 0 \tag{7.23}$$

Equilibrium of moments results in point A

$$N_{U_4} h - F_1(l_1 + l_2 + l_3) - F_2(l_2 + l_3) - F_3 l_3 = 0 \tag{7.24}$$
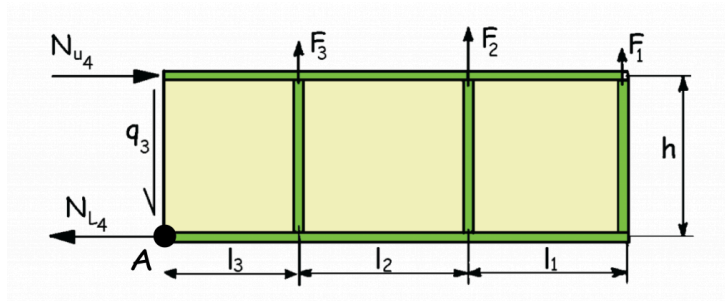
Figure 7.18
Global equilibrium between external forces and reaction forces. (TU Delft, n.d., 7-18.jpg. Own Work.)

Once global equilibrium is obtained, the problem may be dealt with in detail. The problem is then sectioned into separate shear webs with the related caps. Because the load is applied at the end of the spar, while reaction forces apply to the clamped side of the spar, the analysis will be performed from the spar end in the direction of the spar root.
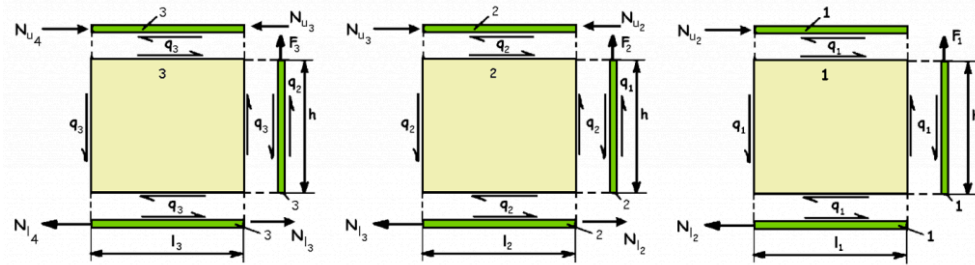

Figure 7.19
The problem of Figure 7.18 broken up into separate sections. (TU Delft, n.d., 7-19.jpg. Own Work.)

First, vertical equilibrium must be provided between the external load F_1 and the shear web. Subsequently, the horizontal equilibrium and equilibrium of moments can be formulated

$$F_1 = q_1 h$$

$$N_{U_2} = q_1 l_1 = \frac{F_1}{h} l_1 \qquad (7.25)$$

$$N_{L_2} = q_1 l_1 = \frac{F_1}{h} l_1$$

Here, q_1 is the shear flow in web plate 1.

Similarly, the equilibrium can be formulated for the second shear web and upper and lower caps:

$$F_2 = q_2 h - q_1 h$$

$$N_{U_3} = N_{U_2} + q_2 l_2 = \frac{F_1}{h} l_1 + \frac{F_1 + F_2}{h} l_2 \qquad (7.26)$$

$$N_{L_3} = N_{L_2} + q_2 l_2 = \frac{F_1}{h} l_1 + \frac{F_1 + F_2}{h} l_2$$

And for the third shear web and upper and lower caps:

$$F_3 = q_3 h - q_2 h$$

$$N_{U_4} = N_{U_3} + q_3 l_3 = \frac{F_1}{h} l_1 + \frac{F_1 + F_2}{h} l_2 + \frac{F_1 + F_2 + F_3}{h} l_3 \qquad (7.27)$$

$$N_{L_4} = N_{L_3} + q_3 l_3 = \frac{F_1}{h} l_1 + \frac{F_1 + F_2}{h} l_2 + \frac{F_1 + F_2 + F_3}{h} l_3$$

From this analysis it can be observed that the transverse shear force is building up towards the spar root. At the first shear web near the wing tip, the transverse shear force D_1 is equal to F_1, while at the second shear web, the transverse shear force D_2 is equal to $F_1 + F_2$ etc. As a consequence, the transverse shear force at location n (or shear web n) can be generalized as

$$D_n = F_1 + F_2 + \cdots + F_n = \sum_1^n F_n \qquad (7.28)$$

The relation between the transverse shear force and the shear flow in the web plate can be derived from equations (7.25) to (7.27) according to:

$$F_1 = q_1 h \Rightarrow q_1 = \frac{F_1}{h}$$

$$F_2 = q_2 h - q_1 h = q_2 h - F_1 \Rightarrow q_2 = \frac{F_1 + F_2}{h} \qquad (7.29)$$

$$F_3 = q_3 h - q_2 h = q_3 h - F_2 - F_1 \Rightarrow q_3 = \frac{F_1 + F_2 + F_3}{h}$$

Thus, the shear flow in each web is described by:

$$q_n = \frac{D_n}{h} \qquad (7.30)$$

Similarly, it follows that the normal forces in the upper and lower caps at the location of the vertical stiffener is given by

$$N_{m+1} = \frac{1}{h} \sum_{n=1}^{m} D_n l_n \qquad (7.31)$$

As explained in section 6.3.2, the constant shear flow in the shear webs results in an increase in normal forces in the spar caps, because the caps transfer the shear flow into normal forces. Thus equation (7.31) describes the normal forces at the location of the vertical stiffener, the normal forces in-between the stringers require some additional analysis.

Figure 7.20
Upper spar cap of web 2 in Figure 7.19 sectioned at location x. (TU Delft, n.d., 7-20.jpg. Own Work.)

Consider the upper spar cap in web plate 2 as illustrated in Figure 7.20. Equilibrium for the side of the spar cap indicated by 'A' can be given by

$$N_{U_3} - N_{U_x} - q_2 x = 0 \qquad (7.32)$$

Similarly, equilibrium for the side indicated with 'B' is obtained with

$$N_{U_x} - N_{U_2} - q_2(l_2 - x) = 0 \qquad (7.33)$$

With equations (7.30) and (7.31) both equations (7.32) and (7.33) result in

$$N_{U_x} = \frac{D_2}{h}(l_2 - x) + \frac{D_1}{h}l_1 \qquad (7.34)$$

This equation illustrates that the normal forces increase linearly from outboard to inboard.

7.5.2 Bending moments

The bending moments at location x in web 2 of the spar can be derived from equation (7.34)

$$N_{U_x} h \equiv M_x = D_2(l_2 - x) + D_1 l_1 \tag{7.35}$$

For web 2 in the spar one can thus obtain that

$$\frac{dM_x}{dx} = -D_2 \tag{7.36}$$

Which is valid on every location x on the spar. Thus equation (7.36) can be generalized as

$$\frac{dM_x}{dx} = -D_x \tag{7.37}$$

7.5.3 Bending of wing spar

Thus once a spar is loaded in bending by external forces F_n the transverse shear forces are known with equation (7.30) and the normal forces in the spar caps are known as

$$N = \frac{M}{h} \tag{7.38}$$

This enables the determination of the transverse shear force and moment diagram as illustrated in Figure 7.21.
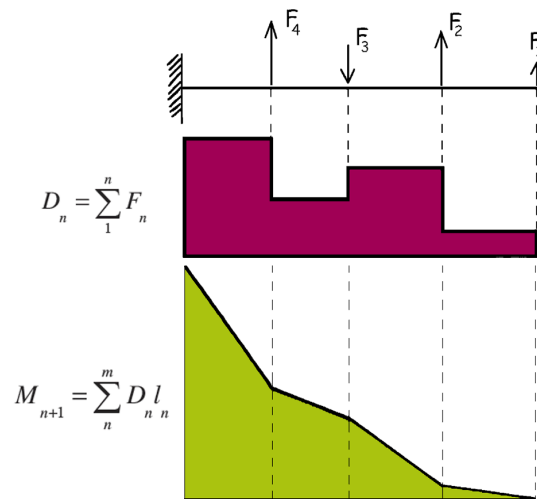

Figure 7.21
Bending of wing spar; transverse shear force and moment diagram. (TU Delft, n.d., 7-21.jpg. Own Work.)

In case of a wing structure, where not only the lift is considered as distributed forces rather than concentrated forces, but in addition also the weight of fuselage and engines is considered, the transverse shear and moment diagrams will look similar to Figure 7.22.
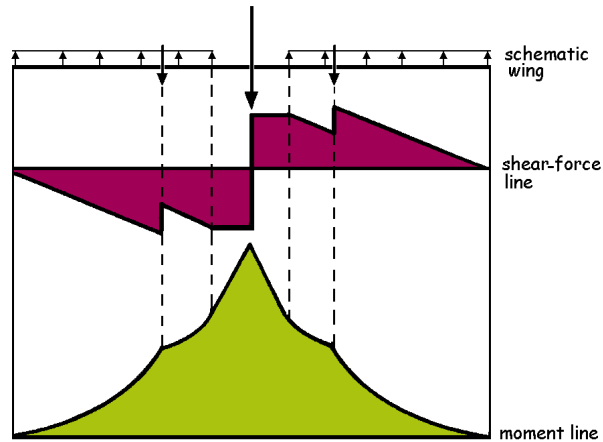

Figure 7.22
Transverse shear force and moment diagram of aircraft wing. (TU Delft, n.d., 7-22.jpg. Own Work.)

It should be noted, that the transverse shear line linearly increases or decreases due to the distributed forces, which implies for the moment line a non-linear increase or decrease.

The shear stress in the webs is given by

$$\tau_x = \frac{q_x}{t_x} = \frac{D_x}{ht_x} \tag{7.39}$$

While the normal stress in the spar caps is given by

$$\sigma_x = \pm\frac{N_x}{A_x} = \pm\frac{M_x}{hA_x} \tag{7.40}$$

Here, the parameters hA_x are called the moment of resistance W in a spar.

Introduction to Aerospace Structures and Materials

Dr.ir. R.C. (René) Alderliesten

This book provides an introduction to the discipline of aerospace structures and materials. It is the first book to date that includes all relevant aspects of this discipline within a single monologue. These aspects range from materials, manufacturing and processing techniques, to structures, design principles and structural performance, including aspects like durability and safety. With the purpose of introducing students into the basics of the entire discipline, the book presents the subjects broadly and loosely connected, adopting either a formal description or an informal walk around type of presentation. A key lessons conveyed within this book is the interplay between the exact science and engineering topics, like solid material physics and structural analysis, and the soft topics that are not easily captured by equations and formulas. Safety, manufacturability, availability and costing are some of these topics that are presented in this book to explain decisions and design solutions within this discipline.

Dr.ir. R.C. (René) Alderliesten
TU Delft | Faculty of Aerospace Engeneering

Dr. Alderliesten obtained his MSc and PhD degree both at TU Delft, and holds since 2012 the position of associated professor within the department of Aerospace Structures and Materials at the faculty of Aerospace Engineering, TU Delft. His expertise is fatigue and damage tolerance of metals, composites and hybrid materials, with the emphasis on proper understanding the physics of damage growth. Dr. Alderliesten introduces Aerospace Structures & Materials in the first semester of the BSc curriculum, while teaching Fatigue of Structures & Materials in the first semester of the MSc both at TU Delft and at the University di Bologna.

TUDelft

ISBN 978-94-6366-071-4

9 789463 660754